Synthesis and Enhanced Photocatalytic Activity of Ce-Doped Zinc Oxide Nanorods by Hydrothermal Method

N Aisah[1], D Gustiono[1], V Fauzia[2], I Sugihartono[3] and R Nuryadi[1]

[1]Agency for the Assessment and Application of Technology, Serpong, Indonesia
[2]Department of Physic, Universitas Indonesia, Depok, Indonesia
[3]Department of Physic, State University of Jakarta, Jakarta, Indonesia

Email: nuning.aisah@bppt.go.id

Abstract. Zinc oxide (ZnO) is a n-type semiconductor material which has a wide direct band gap energy of ~ 3.3 eV, and other interesting optical properties, hence it's potentially applied to various fields such as electronics, optoelectronics, sensors, photonic devices, and also photocatalyst. Dopant in ZnO nanostructures is an effective way to improve ZnO's structural properties in various applications. In this study, undoped and Ce doped ZnO nanorods were synthesized on ITO coated glass substrates by ultrasonic spray pyrolysis for seeding deposition and hydrothermal methods at a temperature of 95 ^{0}C for 2 hours for growth. X-ray diffraction, field emission scanning electron microscopy (FESEM), UV-VIS and Photoluminescence spectroscopy were used to characterize the crystal structure, surface morphology and optical properties of ZnO nanorods and the photocatalytic activity test for methylene blue degradation. The experimental results showed that 3% Cerium dopant has produced hexagonal morphology ZnO nanorod growing more uniform on (002) crystal planes, increased the intensity of ultraviolet absorbance thereby increase the degradation speed of methylene blue.

1. Introduction

Zinc oxide is n-type semiconductor which has wide and direct band gap energy of ~ 3.3 eV at room temperature, large exciton binding energy of 60 meV, excellent thermal stability, high electron mobility and specific electrical and optical properties [1], [2]. ZnO can be used for some application such as electronics, optoelectronics, sensors, photonic devices and photocatalyst.

ZnO nanorod is one of the nanostructure materials most widely synthesized due to its large surface area. ZnO nanostructures were fabricated by various methods such as thermal evaporation, vapor phase deposition, pulsed laser deposition that requires the complex processes, sophisticated equipment and high vacuum [3]. Then, the chemical based approaches such as the ultrasonic spray pyrolysis (USP) [4], [5], sol-gel [6] and hydrothermal methods [2] show the advantages i.e. it can be operated at low temperature, low pressure with simple operation.

Doping of ZnO nanostructures is one effective way to improve the structural properties of ZnO for various applications. In particular, doping ZnO with rare earth materials is of interest in tailoring its optical properties [7]. One of the rare earth metal elements that commonly known as the lanthanide group of the periodic system is cerium. The previous researches such as Lang *et al*. [8] have observed that the Ce dopant has a strong effect on the structure and PL characteristics of ZnO nanorods. Murugadoss *et al.* also have investigated the various doping concentrations of Ce that showed strong

absorption and emission in a visible region of UV-vis and PL spectra [9]. While Nidhi Sinha *et al.* reveal that Ce doping resulted in a shift of XRD peaks to higher angles, decreased size of nanorods, lowered the band gap of ZnO and increased in the intensity of green emission peak in PL [10]. As can be seen from extensive searching that there is only limited literature available about the utilization of Ce doped ZnO nanorods for the treatment of organic contaminants via photocatalysis. One promising approach is to utilize a photocatalytic process from semiconductors nanomaterial such as TiO_2 and ZnO. Selection of ZnO as a photocatalyst due to the wider energy band gap so it can absorb more light [11].

In this work, we synthesized and characterized the undoped and Ce doped ZnO nanorods on Indium Tin Oxide coated glass substrates with USP and hydrothermal method and then investigated the optical properties and the photocatalytic activity. The ultrasonic spray pyrolysis (USP) has many advantages such as low cost, deposition equipment that is simple and easy fabrication of large area films. USP is a method of fabricating a thin layer based on the thermal decomposition of the precursor solution is sprayed through an ultrasonic nozzle above the surface of the substrate which has been heated [4], [12], [13]. Nanorod growth by hydrothermal method is expected to produce nanorod with minimal defects, high crystallinity, good homogeneity as well as having a special morphology and metastable phase thermodynamics [14].

2. Experimental details

2.1. Synthesis of ZnO Nanorods

Firstly, ZnO seed layers were deposited on ITO-coated glass substrates with ultrasonic spray pyrolysis technique. The seed solution was 0.2 M zinc acetate dihydrate $Zn(CH_3COO)_2.2H_2O$ (Merck) that was diluted in distilled water and placed into a nebulizer. The fine droplets were atomized with ultrasonic wave 1.65 MHz and sprayed onto the substrate at a distance of 10 cm. During the spraying process for 10 minutes, the substrates were heated at a temperature of 450 ^{0}C on the hotplate and then cooled down to room temperature. The second step is the growth of nanorods by the hydrothermal method. The growth solution consists of 0.1M Zinc nitrate tetrahydrate $Zn(NO_3)_2.4H_2O$ (Merck) and 0.1M hexamethylenetetramine (HMT) $C_6H_{12}N_4$ (Sigma Aldrich) with the molar ratio 1:1 and then mixed using a magnetic stirrer for 10 minutes at room temperature. Then, 3mol% of cerium nitrate hexahydrate $Ce(NO_3)_3.6H_2O$ (Sigma Aldrich) was added into the growth solution and kept on stirring until the temperature reached 60 ^{0}C. In order to grow the Ce-doped ZnO nanorods, the substrates were then immersed in this solution and heated at a temperature of 95 ^{0}C for 2 hours in oven. After that, the samples were rinsed with distilled water several times and dried at 80 ^{0}C for 30 minutes.

2.2. Characterization

The surface morphology of ZnO nanorods was determined by field emission scanning electron microscopy (FESEM) INSPECT F50. The crystalline structures of the samples were characterized by Shimadzu X-ray Diffraction 7000 Maxima X with CuKα (1.54060 Å) X-ray source using a current of 30 mA and a voltage of 40 kV. The UV-Vis absorption spectrum analysis was performed by Thermo Fisher Scientific GENESYS 10S UV-vis Spectrometer and the Hitachi UV-vis Spectrometer U-3900H for the diffuse reflectance mode. The room-temperature photoluminescence (PL) measurements were carried out using a FLS920 (Edinburg Instruments).

2.3. Photocatalytic Experiments

The photocatalytic activity was investigated by means of the degradation of methylene blue (MB) in an aqueous solution. The ZnO nanorods were placed in a beaker that contained 3mL of 1×10^{-5}MMB and they were then irradiated with backlight lamps. After irradiating for 0, 10, 20 and 30 min, the concentration of residual MB was determined by a UV–vis spectrophotometer.

3. Results and discussion

3.1. Surface Morphology of ZnO Nanorods

Figure 1 (a) and (b) shows the FESEM images of undoped ZnO and Ce-doped ZnO nanorods. It can be seen that the undoped ZnO nanorod has a sharp tip-shaped like a needle. Furthermore, the rod diameter is small with an average of 125 nm. The ZnO nanorod with Cerium dopant is generally hexagonal in shape with an average diameter is large enough about 340 nm. This phenomenon shows that the cerium dopant influences the direction and shape of the nanorods growth. This result was slightly bigger than the result obtained from the same methods in previous researches which the diameter rod produced were in the range of 100-200 nm [1], [8], [15], [16].

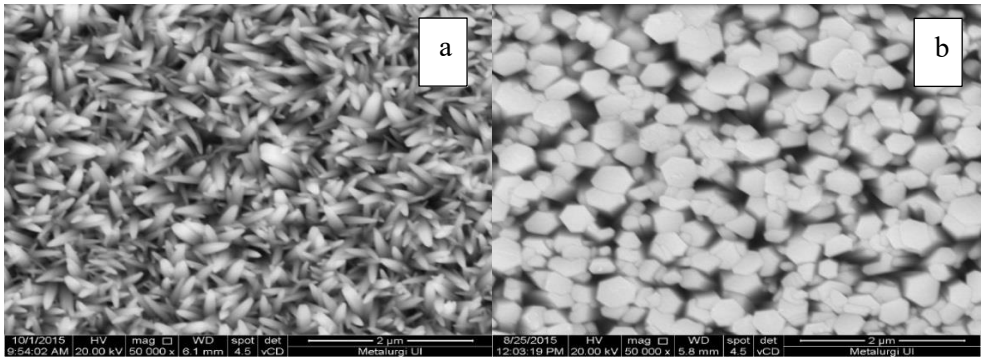

Figure 1. FESEM images of (a) undoped and (b) Ce-doped ZnO nanorods.

3.2. XRD analysis

The X-ray diffraction patterns of undoped Zno and Ce-doped ZnO nanorods are shown in figure 2. The diffraction peaks, i.e. (100), (002), (101), (102) and (103) are similar to bulk ZnO and correspond to hexagonal wurtzite ZnO (ICSD No. 98-005-7478). In addition to ZnO phase, there are other peaks at angles of 30.27, 35.17 and 50.98 which indicate the indium oxide phase derived from the ITO substrate. Preferred orientation of ZnO crystal along (002) and (013) indicates the direction of the crystal growth perpendicular to the substrate surface which is in agreement with the results of SEM morphology in figure 1. For Ce-doped ZnO, there is no diffraction peaks of the phases containing Ce were found in the samples which indicated that Ce^{3+} ions substituted the Zn^{2+} sites or interstitial sites in ZnO lattice.

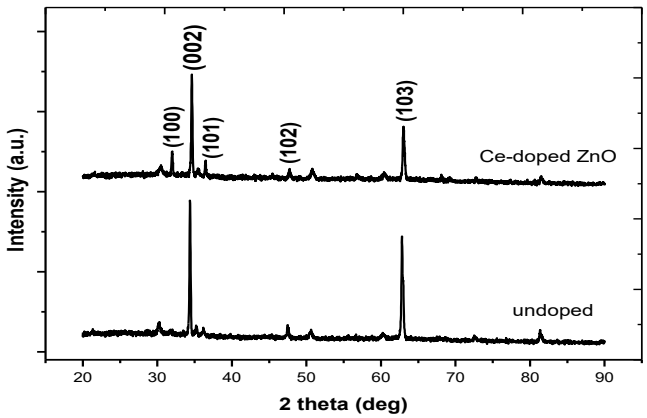

Figure 2. XRD patterns of undoped and Ce doped ZnO.

The diffraction peaks (002) have shifted from 34.40^0 to 34.60^0 after the doping of 3 mol% Ce. The addition of Cerium decreased the intensity of (002) and (103) planes, the full width at half maximum

(FWHM) also widened from 0.14 into 0.15 and the crystallite size also decreased from 84 nm into 74 nm. Decreasing the intensity and widening of FWHM indicates a slight decrease in crystallinity of ZnO nanorods.

The lattice parameters of Ce-doped ZnO nanorods (a = 3.2530, c = 5.2132) increased compared with the undoped one (a = 3.2492, c = 5.2027). It indicates that Ce ions have been incorporated into the ZnO lattice because the ionic radius of Ce^{3+} (1.034 Å) is much bigger than that of Zn^{2+} (0.74 Å).

3.3. Optical properties of ZnO nanorods

Absorption and transmittance spectra of ZnO nanorod can be seen in figure 3. From the absorption spectra, the curve dropped sharply in a range of 375 nm, known as the absorption edge relating to band gap energy of ZnO nanorod samples. Figure 3 (a) exhibits the absorption edge of ZnO nanorod at 373 nm then slightly shifted to 365 nm for Cerium doped. In the sample of 3% Cerium doped ZnO, the shift is followed by an increase in the UV absorption intensity. In general, an increase in the concentration of Cerium dopant will be decreasing the intensity of the absorbance in the visible region. Increasing the intensity of absorption in the UV region is also obtained by N.Sinha et. al. which used 1mol% cerium doped [10].

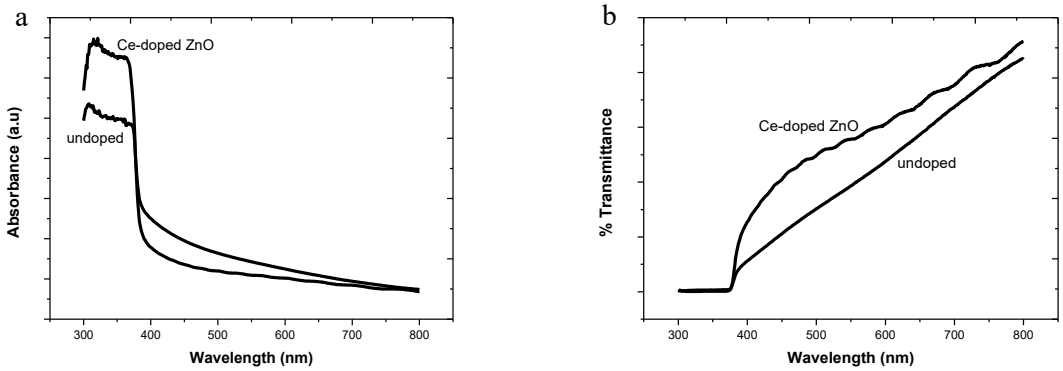

.

Figure 3. UV-vis absorption spectra of undoped ZnO and Ce-doped ZnO (a), transmittance of undoped ZnO and Ce-doped ZnO (b).

The transmittance spectra of ZnO nanorods are shown in figure 3(b). The transmittance in the visible light region was increased for Ce-doped ZnO nanorods, while the transmittance in UV region was decreased.

3.4. Diffuse reflectance spectra

The direct band gap energy was calculated by the diffuse reflectance spectrum using Kubelka-Munk formulation and then transferred into Tauc plot as shown figure 4 and figure 5.

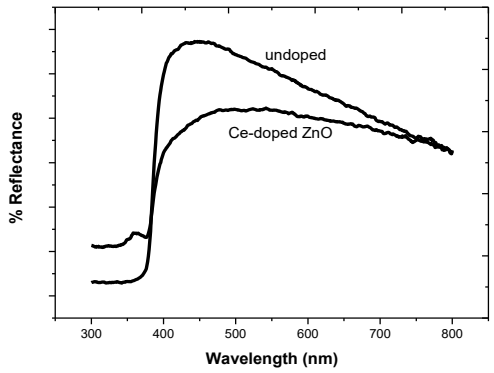

Figure 4. UV-vis diffuse reflectance spectra of ZnO and Ce-doped ZnO

The band gap energy of undoped ZnO nanorods was 3.23 eV and decreased into 3.18 eV after Ce doping. The change of band gap energy may be due to the new energy levels of cerium in ZnO lattice.

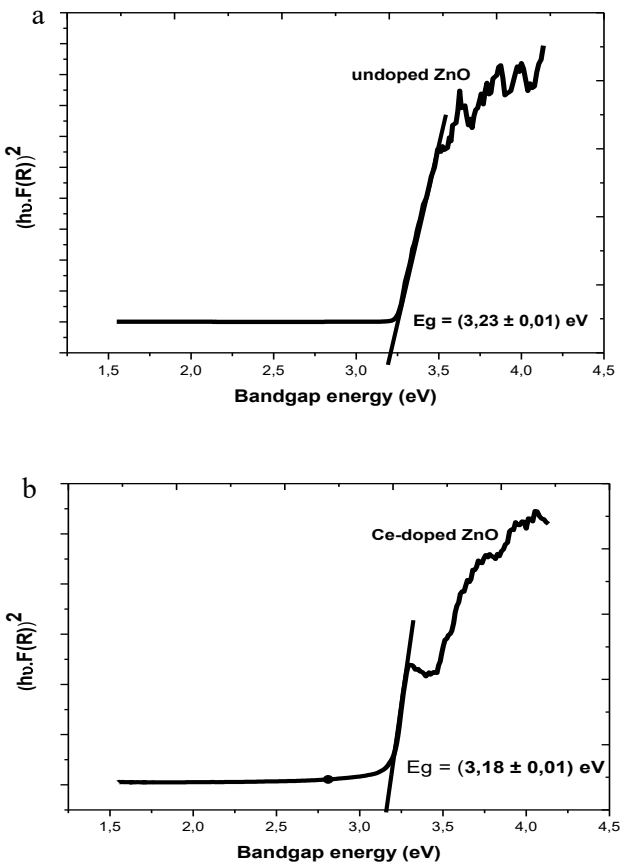

Figure 5. Tauc plot of (a) undoped ZnO. (b) Ce-doped ZnO.

3.5. Photoluminescence spectra

The room temperature PL spectra of undoped ZnO and Ce-doped ZnO nanorods is shown in figure 6. The PL spectra of undoped ZnO exhibits stronger near-band-edge (NBE) emission centered at a wavelength of 398 nm. The UV emission results from the recombination of free or bound exciton indicate the highest crystal quality of the material. It is also observed there is a broad emission band centered at a wavelength of 620 nm. This broad green emission peak is usually associated with the presence of defect levels in the band gap such as oxygen vacancies, zinc vacancies and interstitial zinc ion vacancies [5], [10], [17], [18]. The enhanced intensity of the green emission attributed to the increase of oxygen vacancy introduced by the existence of ce impurities in ZnO nanorods [8].

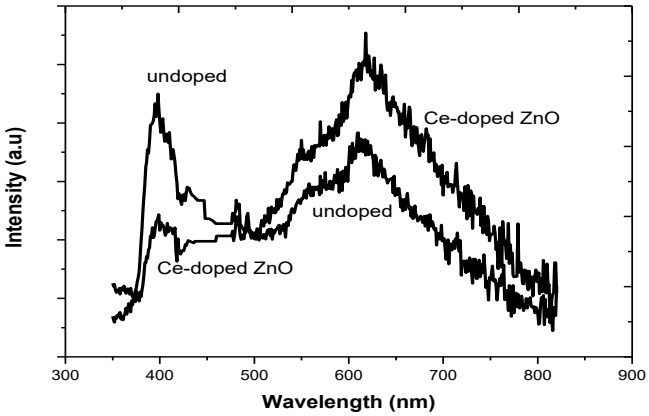

Figure 6. PL spectra of undoped ZnO and Ce-doped ZnO

3.6. Photocatalytic degradation of methylene blue

Figure 7 shows absorption spectra of the MB solution under a UV light irradiation using the ZnO nanorods. Quantitative degradation of methylene blue is shown at 597 nm as absorption peak.

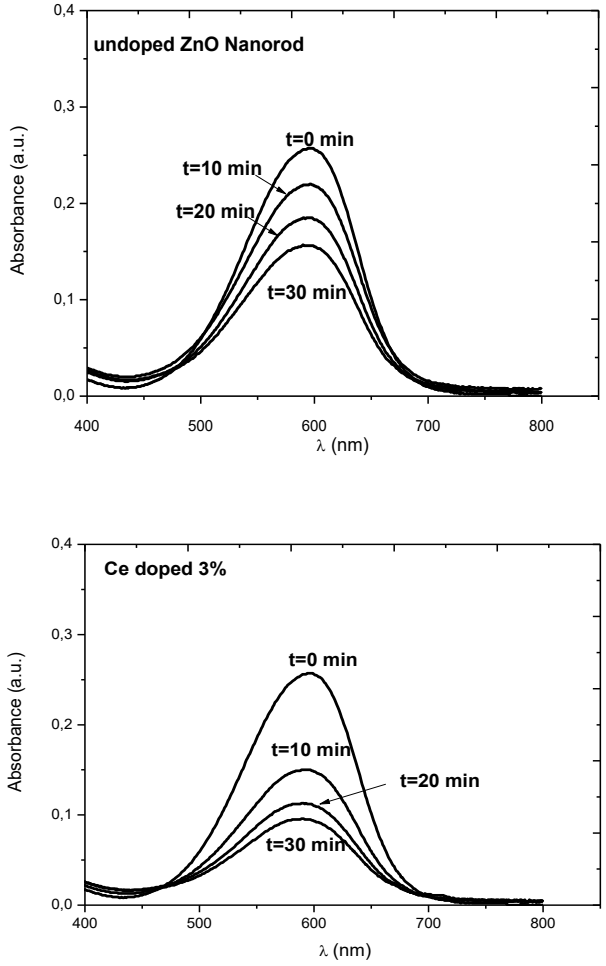

Figure 7. Absorbance spectra of MB by ZnO nanorods photocatalytic activity

The absorbance decreases by the increase of the irradiation time. The degradation of MB was calculated by the following equation (1):

$$\text{Degradation (\%)} = [(A_0-A_t)/A_0] \times 100 \quad (1)$$

where A_t is the absorbance at 597 nm of the MB solutions after irradiation in selected time, and A_0 is the absorbance at 597 nm of the MB solutions before irradiation.

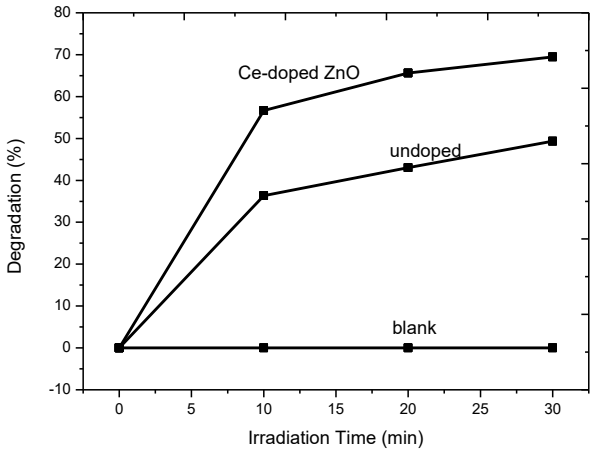

Figure 8. Degradation of MB aqueous solution with ZnO nanorods under UV light irradiation

Figure 8 shows the degradation spectra of MB when treated in the presence of ZnO nanorods photocatalysts. It can be seen that the degradation percentage under undoped Ce is 49% after 30 min of irradiation whereas 69% degradation was achieved in the presence of 3% ce doped ZnO after 30 min of exposure to UV light indicating the photocatalytic performance of 3% Ce doped ZnO has been running well.This result may be related to the lowest bandgap energy of Ce doped ZnO nanorod, thus widening the spectrum of UV light can excite the electrons into the conduction band which generates electrons and holes with higher numbers. Faisal *et al.* [19] mentioned that cerium acts as a "warehouse" of electrons and inhibitors of electron-hole pair recombination in producing light so as to increase the ability of the photocatalytic of ZnO nanorod.

4. Conclusions

The Ce-doped ZnO nanorods were synthesized by low-temperature hydrothermal process. In FESEM, the size increase of nanorods was obtained for Ce doped ZnO and Cerium dopant influence the direction and shape of the nanorods. Ce doping resulted in decreasing of the intensity of (002) and (103) planes and widening of FWHM, it indicate a slight decrease in crystallinity of ZnO nanorods. Increasing the concentration of Cerium dopant decreases the intensity of the absorbance in the visible region. The band gap energy of undoped ZnO nanorods was 3.23 eV that was decreased into 3.18 eV after Ce doping. The change of band gap energy may be due to the new energy levels of Cerium in ZnO lattice. The enhanced intensity of the green emission attributed to the increase of oxygen vacancy introduced by the existence of Ce impurities in ZnO nanorods. Photocatalytic experiment ZnO nanorods to degrade methylene blue for 30 minutes showed that 3% Ce doped ZnO have the fastest degradation ability of MB due to the highest intensity of absorbance and the lowest bandgap energy making it more effective for generating electrons and holes with significant amount that required to degrade methylene blue.

References

[1] Chang C, Lin C, Chen J, and Hsu M 2014 Ce-doped ZnO nanorods based low operation

temperature NO_2 gas sensors *Ceram Int.* **40** 10867
[2] Liu Y and Gao W 2015 Growth process, crystal size and alignment of ZnO nanorods synthesized under neutral and acid conditions *J. Alloys Compd.* **629** 84
[3] Yang L, Zhao Q, Willander M and Yang J H 2009 Effective way to control the size of well-aligned ZnO nanorod arrays with two-step chemical bath deposition *J. Cryst. Growth* **311** 1046
[4] Ma H L, Liu Z W, Zeng D C, Zhong M L, Yu H Y and Mikmekova E 2013 Nanostructured ZnO films with various morphologies prepared by ultrasonic spray pyrolysis and its growing process *Appl. Surf. Sci.* **283** 1006
[5] Sri P 2014 Structural and Optical Properties of Cerium doped Zinc Oxide thin films using spray pyrolysis *J. NanoSci. NanoTechnol.* **2** 34
[6] Benramache S, Rahal A, and Benhaoua B 2014 The effects of solvent nature on spray-deposited ZnO thin film prepared from Zn $(CH_3COO)_2$, $2H_2O$ *Opt. - Int. J. Light Electron Opt.* **125** 663
[7] Yang J, Gao M, Yang L, Zhang Y, Lang J, Wang D, Wang Y, Liu H, and Fan H 2008 Low-temperature growth and optical properties of Ce-doped ZnO nanorods *Appl. Surf. Sci.* **255** 2646
[8] J. Lang, Q. Han, J. Yang, C. Li, X. Li, L. Yang, Y. Zhang, M. Gao, D. Wang, and J. Cao 2010 Fabrication and optical properties of Ce-doped ZnO nanorods *J. Appl. Phys.* **107** 2
[9] G. Murugadoss, R. Jayavel, and M. Rajesh Kumar 2015 Structural and optical properties of highly crystalline Ce, Eu and co-doped ZnO nanorods *Superlattices Microst.* **82** 538
[10] N. Sinha, G. Ray, S. Bhandari, S. Godara, and B. Kumar 2014 Synthesis and enhanced properties of cerium doped ZnO nanorods *Ceram. Int.* **40** 12337
[11] N. Febiana Djaja, Rosari Saleh 2013 Characteristics and photocatalytics activities of Ce-Doped ZnO nanoparticles *Mat. Sci. Appl.* **4** 145
[12] A. Bedia, F. Z. Bedia, M. Aillerie, N. Maloufi, and B. Benyoucef 2015 Morphological and optical properties of ZnO thin films prepared by spray pyrolysis on glass substrates at various temperatures for integration in solar cell *Energy Procedia.* **74** 529
[13] S. Benramache, B. Benhaoua, F. Chabane, and A. Guettaf 2013 A comparative study on the nanocrystalline ZnO thin films prepared by ultrasonic spray and sol–gel method *Opt. - Int. J. Light Electron Opt.* **124** 3221
[14] T. T. Y. Tan 2012 *Rare Earth Nanotecnhology*. Singapore: Pan Stanford Publishing Pte.Ltd.
[15] X. Y. Chen, F. Fang, A. M. C. Ng, A. B. Djurisic, W. K. Chan, H. F. Lui, P. W. K. Fong, C. Surya, and K. W. Cheah 2011 Effect of doping precursors on the optical properties of Ce-doped ZnO nanorods *Thin Solid Films* **520** 1125
[16] G. N. Dar, A. Umar, S. A. Zaidi, A. A. Ibrahim, M. Abaker, S. Baskoutas, and M. S. Al-Assiri 2012 Ce-doped ZnO nanorods for the detection of hazardous chemical *Sensors Actuators, B Chem.* **173** 72
[17] Y.-I. Jung, B.-Y. Noh, Y.-S. Lee, S.-H. Baek, J. H. Kim, and I.-K. Park 2012 Visible emission from Ce-doped ZnO nanorods grown by hydrothermal method without a post thermal annealing process *Nanoscale Res. Lett.* **7** 43
[18] S. Y. Kuo, W. C. Chen, F. I. Lai, C. P. Cheng, H. C. Kuo, S. C. Wang, and W. F. Hsieh 2006 Effects of doping concentration and annealing temperature on properties of highly-oriented Al-doped ZnO films *J. Cryst. Growth* **287** 78
[19] M. Faisal, A. A. Ismail, A. A. Ibrahim, H. Bouzid, and S. A. Al-Sayari 2013 Highly efficient photocatalyst based on Ce doped ZnO nanorods: Controllable synthesis and enhanced photocatalytic activity *Chem. Eng. J.* **229** 225

Acknowledgments
This work was supported by Hibah Publikasi International Terindeks untuk Tugas Akhir Mahasiswa (PITTA) 2016 Universitas Indonesia and grants from the Ministry of Research, Technology and Higher Education of the Republic of Indonesia (Insinas 2016).